ELSEVIER

Contents lists available at ScienceDirect

# Global and Planetary Change

journal homepage: www.elsevier.com/locate/gloplacha





# Enhanced climate variability during the last millennium recorded in alkenone sea surface temperatures of the northwest Pacific margin

Kyung Eun Lee <sup>a,b,\*</sup>, Wonsun Park <sup>c</sup>, Sang-Wook Yeh <sup>d</sup>, Si Woong Bae <sup>b</sup>, Tae Wook Ko <sup>b</sup>, Gerrit Lohmann <sup>e</sup>, Seung-Il Nam <sup>f</sup>

- <sup>a</sup> Department of Ocean Science, Korea Maritime and Ocean University, Busan, South Korea
- <sup>b</sup> Ocean Science and Technology School, Korea Maritime and Ocean University, Busan, South Korea
- <sup>c</sup> GEOMAR Helmholtz Centre for Ocean Research Kiel, 24105 Kiel, Germany
- <sup>d</sup> Department of Marine Science and Convergence Engineering, Hanyang University, ERICA, Seoul 15588, South Korea
- e Alfred-Wegener-Institute, Bremerhaven 27570, Germany
- f Arctic Research Center, Korea Polar Research Institute, Incheon, South Korea

### ARTICLE INFO

# Keywords: Last millennium Common Era Past sea surface temperature Volcanic forcing East Asian summer monsoon North Pacific

### ABSTRACT

Previous studies on surface temperature reconstructions for the last 2000 years (2 k) revealed a long-term cooling trend for the last millennium in comparison to the previous millennium. However, knowledge on the decadal- to centennial-scale variability in sea surface temperature and the underlying governing mechanisms throughout the period is limited. We reconstructed high-resolution continuous sea surface temperature changes over the last 2 k in the northwest Pacific margin based on the alkenone unsaturation index. Our alkenone temperature record revealed enhanced and more rapidly changing climate variability during the last millennium (approximately 1200–1850 Common Era) than during the previous millennium. Cold and hot extremes also occurred more frequently during the last millennium. The enhanced and rapidly changing climate variability appears to be associated with frequent volcanic eruptions and grand solar minima. The reconstructed surface temperature variability tends to be associated with variations in the East Asia summer monsoon and the Pacific Decadal Oscillation, implying that these variations are also enhanced in the last millennium than in the previous millennium.

# 1. Introduction

The network of the Past Global Changes project synthesised surface temperature data for the past 2000 years (herein 2k) to reconstruct regional and global variations (PAGES 2k Consortium, 2013). All of the continental temperature records compiled display a long-term cooling trend beginning at approximately 1200 CE and ending in the nineteenth century, although these past global changes exhibited strong regional differences in timing of cooling (PAGES 2k Consortium, 2013). A global synthesis of sea surface temperatures (SST) also revealed a cooling trend that began earlier and was sustained for a millennium (801–1800 CE) (McGregor et al., 2015). However, due to the issues of scarcity, resolution, continuity, and uncertainty of the SST records, they provided only the 200-year averaged data. Therefore, it was difficult to identify the multi-decadal- and centennial-scale variations in SST over the last 2 k from the records. Even today, a scarcity of high-resolution SST records

over the last  $2\,k$  impedes further progress toward identifying the natural variability itself on multi-decadal and centennial scales, and understanding the relations with climate forcing.

Previous studies on data reconstruction and model simulations tried to identify internal and external forcing associated with the reconstructed temperature variations including parameters of solar irradiance, volcanic activity, land-cover changes, and orbital-driven insolation, and the results suggested that the cooling trend of the ocean surface temperature over the period of 801–1800 CE was not primarily a response to solar forcing but may have been related to the increased frequency of explosive volcanism (McGregor et al., 2015). Recently, Atlantic multi-decadal variability over the past 1200 years was clarified using terrestrial proxy records from the circum-North Atlantic region (Wang et al., 2017) and the results suggested that natural external forcing (volcanic and solar irradiation) explained approximately 30% of the variance observed in the reconstruction on multi-decadal scale, and

<sup>\*</sup> Corresponding author at: Department of Ocean Science, Korea Maritime and Ocean University, Busan, South Korea. E-mail address: kyung@kmou.ac.kr (K.E. Lee).

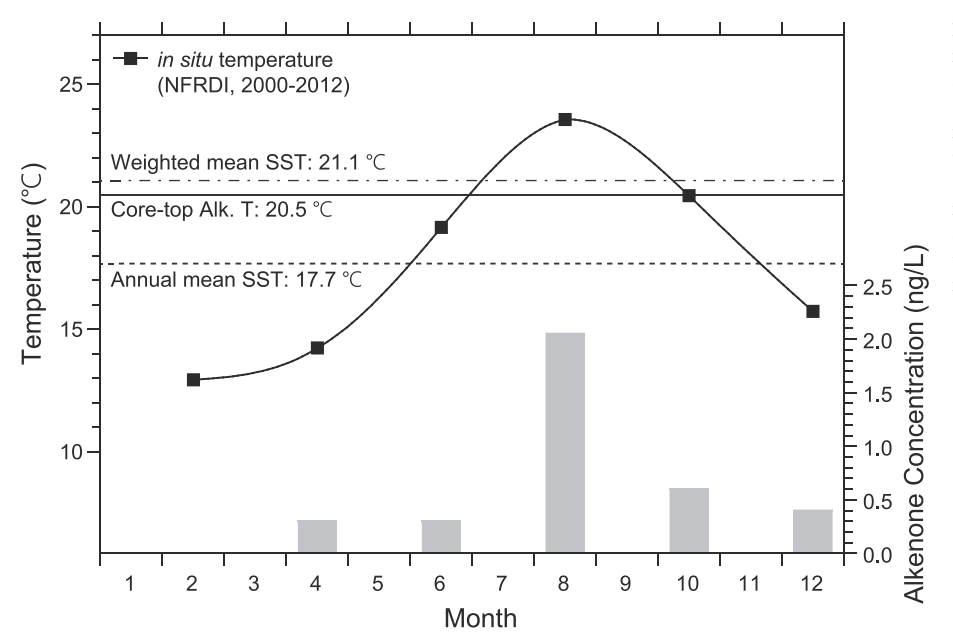


Fig. 1. Bi-monthly records of SST and total  $C_{37}$  alkenone concentration at the core site. The 12-year averaged SST measured *in situ* was from the NFRDI (2000–2012). Total  $C_{37}$  alkenone concentration was measured from suspended surface water particles near the core site for two years (2009–2010) (Lee et al., 2014). The straight line indicates the core-top alkenone temperature. The dashed line indicates the annual mean SST. The dashed-dotted line indicates the annual mean SST, considering the weight of the monthly alkenone concentration.

**Table 1** <sup>14</sup>C ages for the ARA/ES 03–01 GC01 core.

Sample depth (cm)	Material	AMS <sup>14</sup> C Age (yr BP)	Calendar age <sup>a</sup> (CE)	Lab code <sup>b,c</sup>
40–45	Pl. Foram.	$125\pm20$		OS-104642
140–145	Pl. Foram.	$535 \pm 20$	$1767\pm10$	OS-104654
250-255	Pl. Foram.	$670 \pm 25$	$1619\pm18$	OS-104643
280-285	Pl. Foram.	$739 \pm 19$	$1565\pm19$	R40157/1
340-345	Pl. Foram.	$820\pm25$	$1453\pm16$	OS-104644
380-386	Pl. Foram.	$1060\pm20$	$1308\pm16$	OS-104645
450-455	Pl. Foram.	$1530\pm25$	$854 \pm 38$	OS-104646
540-545	Pl. Foram.	$2214\pm19$	$145\pm39$	R40157/2

<sup>&</sup>lt;sup>a</sup> Calendar ages were converted from radiocarbon ages using Bacon 2.2 software (Blaauw and Christen, 2011).

that internal dynamic processes may have played a role in the variations instead. In addition, the reconstruction of changes in SST off the coast of Baja California in the eastern subtropical Pacific during the last 2 k revealed discontinuous multi-decadal variability with periodicities similar to instrumental observations of the Pacific Decadal Oscillation (PDO) and a relationship with megadroughts in southwestern North America (O'mara et al., 2019).

To improve our understanding of climate variability, SST reconstruction from the marine paleoclimate archive is essential, but SST data in the western margin of the North Pacific is still lacking. In this study, we examine the extent to which the natural variability in surface temperature has changed over the past 2 k. Instrumental climate records are available only for the last 100 years. In particular, continuous high-resolution SST records prior to the last century are very limited. To overcome this issue, new SST records covering the past 2 k were reconstructed using the marine sediments near the Korean Peninsula. Quantification of past SST changes at high resolution can be used to identify climate variability on multi-decadal and centennial timescales over the past 2 k. Furthermore, the comparisons of the record with climate forcing and other paleoclimatic records, including the East Asian monsoon and SST records from other regions, help to understand relations between major variability in climate system over the past 2 k.

Paleotemperature reconstruction by alkenones is based on the widely accepted hypothesis that haptophyte microalgae produce long chain  $(C_{37})$  alkenones, whose degree of unsaturation changes with seawater

temperature. The relationship between the alkenone unsaturation index (U<sup>K'</sup><sub>37</sub>) and the temperature of seawaters in which the algae grow has been calibrated using results from laboratory culture experiments involving Emiliania huxleyi (e.g. Prahl and Wakeham, 1987; Prahl et al., 1988), and from the results of analysis of surface water and sediments trap samples (e.g. Prahl et al., 1993), and core-top sediment samples (e. g. Müller et al., 1998). In particular, a bi-monthly record of total C<sub>37</sub> alkenone concentrations measured from suspended particles in surface waters near the Korean Peninsula (Lee et al., 2014) confirmed that the calibration equation given by Prahl et al. (1988;  $U^{K'}_{37}=0.034T+0.039$ ) is applicable in this area. In this study, we reconstructed alkenone SST variations from marine sediments with a higher temporal resolution of approximately 2-8 years, constituting the first well-preserved, long, and continuous SST record of the northwestern Pacific margin spanning the past 2 k. The record reveals the characteristics of temporal variations in temperature in the region on multi-decadal to centennial timescales, although age uncertainty should be considered.

# 2. Materials and methods

Bi-monthly SSTs observed *in situ* at the study area over the period of 2000–2012 were collected from a National Fisheries Research and Development Institute (NFRDI) dataset (Fig. 1). The seasonal SST variations were large  $(13–24\,^{\circ}\text{C})$  in the study area. Sea surface salinity ranged from 32.2 psu in summer to 34.4 psu in winter according to the

<sup>&</sup>lt;sup>b</sup> OS indicates the NOSAMS facility at the WHOI, USA.

<sup>&</sup>lt;sup>c</sup> R indicates the Rafter Radiocarbon Laboratory, New Zealand.

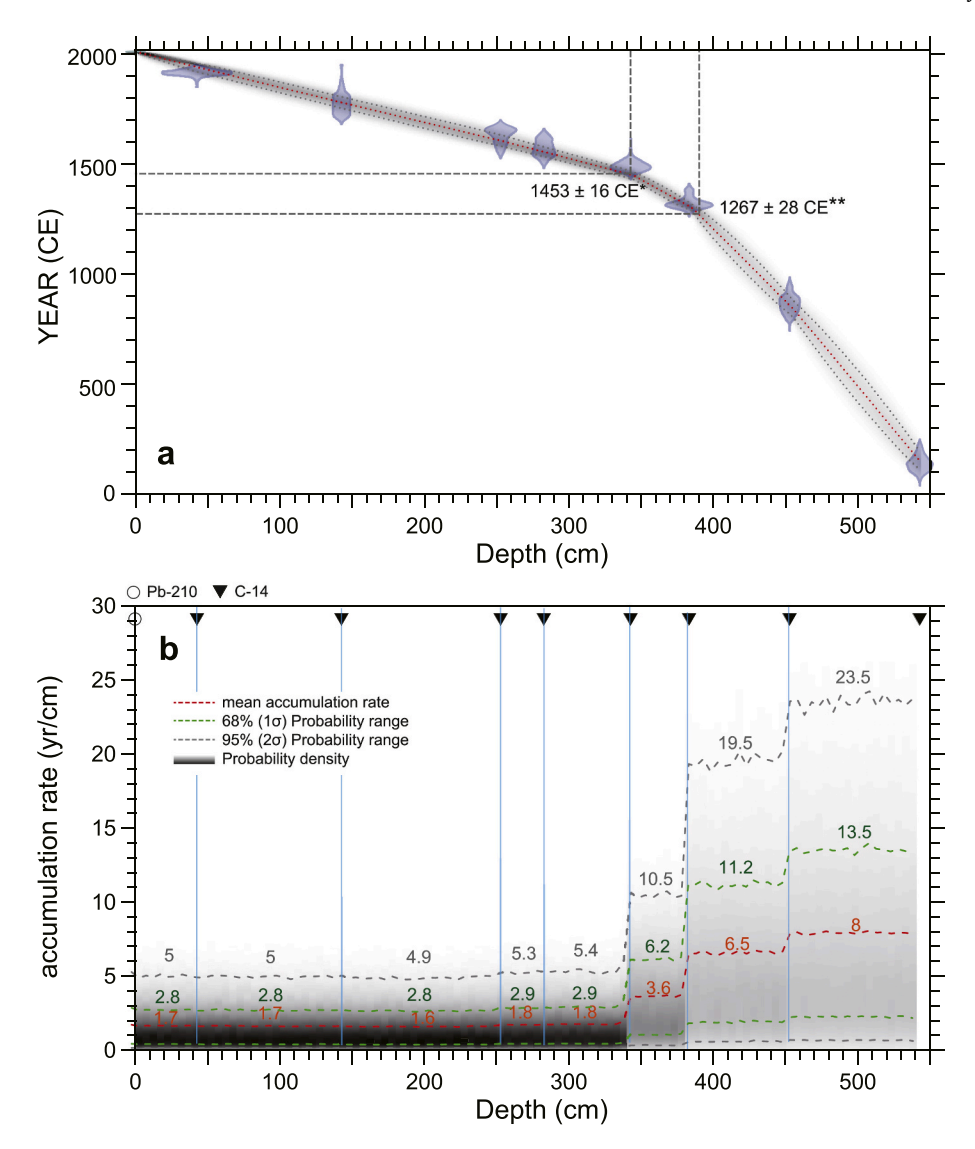


Fig. 2. (a) Age-depth model and (b) accumulation rate of the ARA/ES 03–01 GC01 core, produced using Bacon 2.2 (Blaauw and Christen, 2011). The asterisk (\*) indicates the boundary age of the rapid change in the accumulation rate. The double asterisk (\*\*) indicates the depth and age of the lowest temperature recorded.

**Table 2**  $^{210}$ Pb and  $^{226}$ Ra activities for the NR2018 BC2 core.

Core ID	Sample depth (cm)	Materials	Total <sup>210</sup> Pb (mBq/g) <sup>a</sup>	<sup>226</sup> Ra (mBq/g) <sup>a</sup>	Excess <sup>210</sup> Pb (mBq/g)
NR2018 BC2 #1	1–2	Dry sediment	$445\pm13$	$\textbf{8.4} \pm \textbf{2}$	437
NR2018 BC2 #2	1–2	Dry sediment	$487\pm18$	$13.8\pm3$	473
NR2018 BC2 #2	10–11	Dry sediment	$340\pm19$	$11.7 \pm 3.3$	328
NR2018 BC2 #2	20-21	Dry sediment	$290\pm18$	$10.6 \pm 3.4$	279
NR2018 BC2 #2	30-31	Dry sediment	$273\pm15$	$11.9 \pm 3$	261
NR2018 BC2 #2	42–43	Dry sediment	$197\pm16$	$13\pm3.3$	184

 $<sup>^{\</sup>mathrm{a}}$  Total  $^{\mathrm{210}}\mathrm{Pb}$  and  $^{\mathrm{226}}\mathrm{Ra}$  activities were measured at the at the Korea Basic Science Institute.

NFRDI dataset. Lower salinity occurred in summer, which was due to dilution by summer monsoon river discharge from the adjacent drainage basins of the Korean peninsula and China including the Yangtze River.

A piston core, TY2010 PC4, was collected from a shelf mud deposit off the east coast of the Korean Peninsula during a R/V Tamyang cruise in 2010. The core was  $3.44 \, \text{m}$  long, and was located at the northern part  $(129^{\circ}36'\text{E}, \, 35^{\circ}50'\text{N})$  of the mud deposit at a water depth of 91 m. A

gravity core (ARA/ES 03-01 GC01, 5.45 m in length) was obtained from the same site as that of core TY2010 PC4 during a R/V Araon cruise in 2012. Lithologies and X-ray radiographs of both cores indicated that the marine sediments predominately consist of hemipelagic mud. Because the ARA/ES 03-01 GC01 core contains the longer proxy record, we primarily used this core. However, for the upper section (~1 m), the piston core was used instead. This avoided the potential loss of the upper

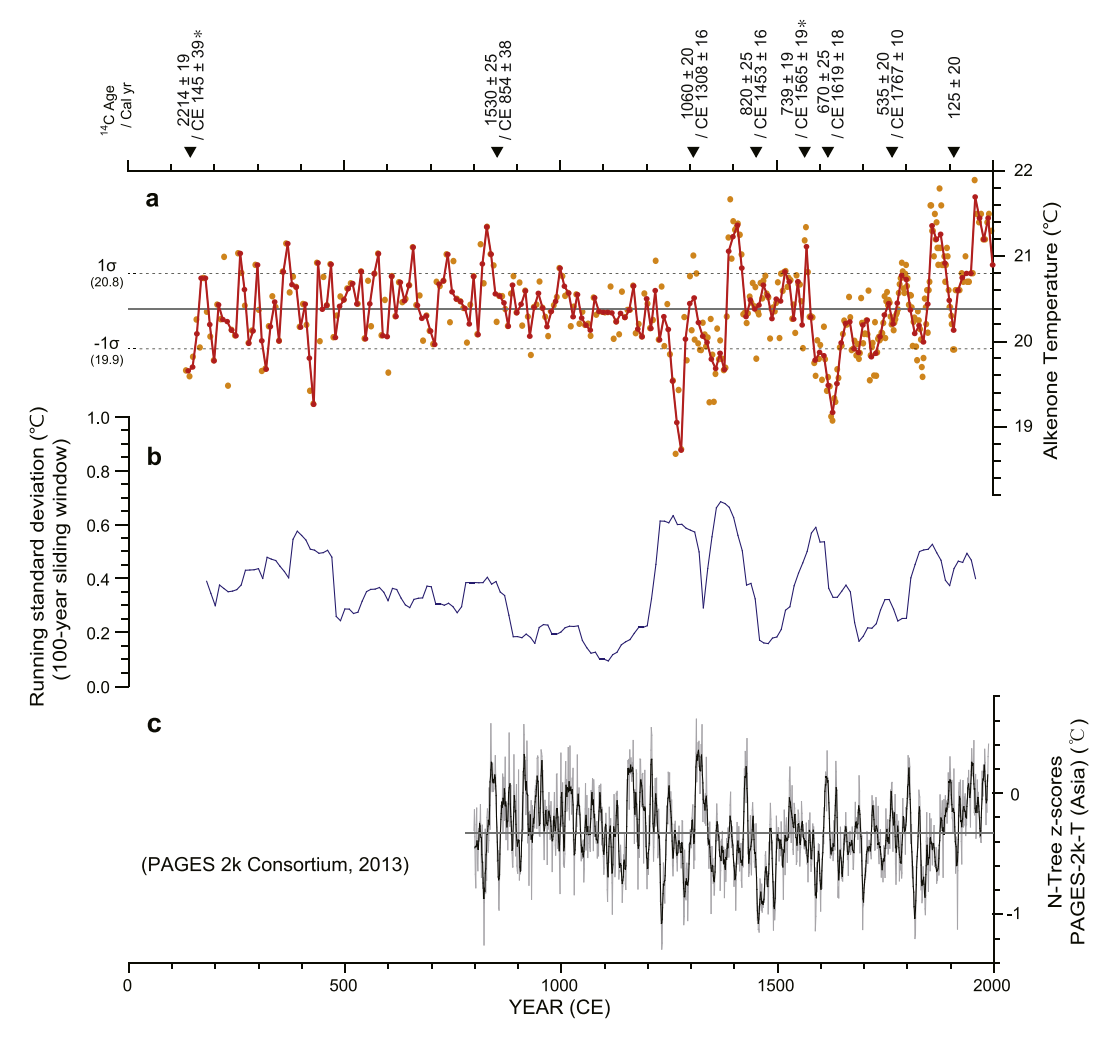


Fig. 3. Time series of (a) alkenone SST versus calendar year in TY2010 PC4 / ARA/ES 03-01 GC01 cores. The thick line indicates the 10-year averaged alkenone SST. Dashed lines represent intervals of the standard deviation, 1σ. Black triangles indicate radiocarbon dates and their uncertainties. (b) Running standard deviation (100-year window) of the alkenone SST. (c) Tree-ring-based air temperatures in Asia (PAGES 2k Consortium, 2013). The horizontal straight line indicates the mean value for 2 k.

portion of the sediment that is more likely to occur when using the gravity coring method (e.g. Skinner and McCave, 2003).

Bulk sediment samples (3 g) were taken from the TY2010 PC4 core at 2-cm intervals for alkenone analysis. For the ARA/ES 03-01 GC01 core, the samples were collected at 2-cm intervals in the upper part of the core (0-340 cm) and at 1-cm intervals in the lower part (340-545 cm). The alkenone analysis was conducted at the Korea Maritime and Ocean University. C<sub>37</sub> alkenones were extracted from the freeze-dried sediment samples. Organic compounds were extracted using an ASE-200 solvent extractor (Dionex Corporation) with a solvent mixture (CH<sub>2</sub>Cl<sub>2</sub>:CH<sub>3</sub>OH, 99:1 v/v) at a high temperature (100 °C) and pressure (1500 psi). The extracts were cleaned via elution with  $3 \times 500 \,\mu L$  CH<sub>2</sub>Cl<sub>2</sub> through a commercial silica cartridge. Saponification was performed at 70 °C for 2 h with 0.1 M KOH. The neutral fraction containing the alkenones was obtained by partitioning into hexane. After being concentrated under N<sub>2</sub>, the final extract was analysed by gas chromatography with an Agilent 7890A chromatograph equipped with a flame ionisation detector and fused-silica capillary column (J&W DB-1,  $60\,\text{m}\times0.32\,\text{mm}$ ). The alkenone temperatures were calculated using the alkenone unsaturation index ( $U^{K'}_{37} = [C_{37:2}] / ([C_{37:2}] + [C_{37:3}])$ ) and the calibration equation given by Prahl et al. (1988;  $U_{37}^{K}=0.034T+0.039$ ). A new calibration,

BAYSPLINE (Tierney and Tingley, 2018), was also applied to calculate seawater temperatures from the  $U^K_{37}$  values. BAYSPILNE produced the exact same SST estimates as those produced using the calibration method of Prahl et al. The reproducibility of the alkenone temperatures for replicate samples of a homogeneous marine sediment laboratory standard run during this project was better than  $\pm 0.1\,^{\circ}$ C ( $n=27,\,1\sigma$ ). Duplicate analyses on ARA/ES 03-01 GC01 gave results within  $\pm 0.2\,^{\circ}$ C ( $n=50,\,1\sigma$ ).

The ARA/ES 03–01 GC01 core ages were determined via radiocarbon dating (Table 1 and Fig. 2). Accelerator mass spectrometry (AMS)  $^{14}\mathrm{C}$  dates of planktonic foraminifera were measured at the Rafter Radiocarbon Laboratory, New Zealand (at two depths) and the National Ocean Sciences AMS (NOSAMS) facility at the Woods Hole Oceanographic Institution (WHOI), USA (at six depths). Although the dates were measured by two different institutes, the results were extremely consistent. An age-depth model was constructed using the Bacon 2.2 package in R (Blaauw and Christen, 2011) (Fig. 2). Bacon simulates the accumulation rates of core sediments based on Bayesian statistics and calculates the ages and uncertainties (1 $\sigma$ ) of sediment deposits. The results of the  $^{210}\text{Pb}$  dating of the box core NR2018 BC2 sediments (129°35.4′E, 35°52′N) collected near the ARA/ES 03–01 GC01 core are

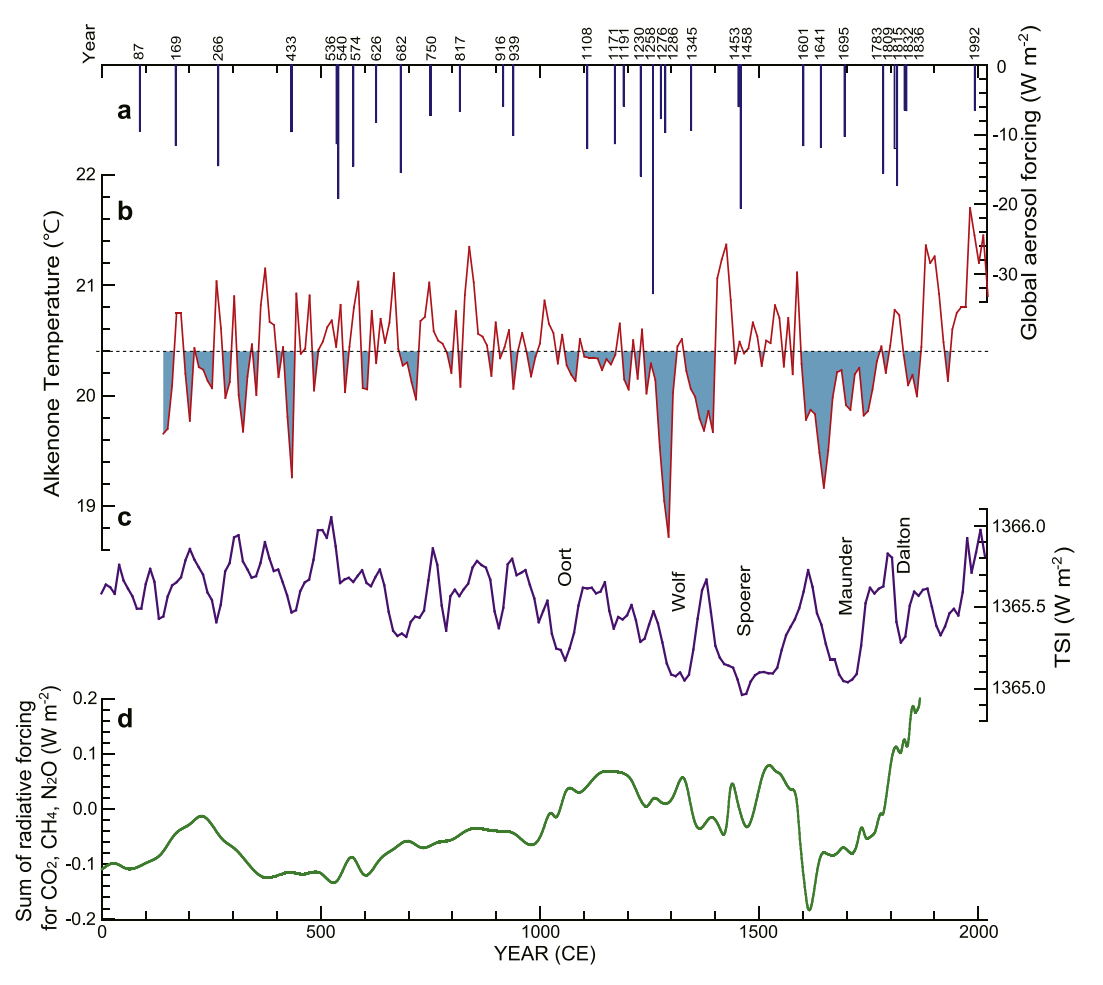


Fig. 4. Time series of (a) the 40 largest global volcanic aerosol forcings (Sigl et al., 2015), (b) alkenone-based SST estimates from TY2010 PC4 / ARA/ES 03–01 GC01 cores, (c) total solar irradiance forcing (Roth and Joos, 2013), and (d) greenhouse gas forcing (MacFarling Meure et al., 2006; Joos and Spahni, 2008). The horizontal dashed line indicates the mean SST value for 2 k.

presented in Table 2. The  $^{210}$ Pb and  $^{226}$ Ra activities were measured at the Korea Basic Science Institute (KBSI). The observed excess  $^{210}$ Pb activities in the NR2018 BC2 core indicate that the core-top surface sediments are modern-day sediments.

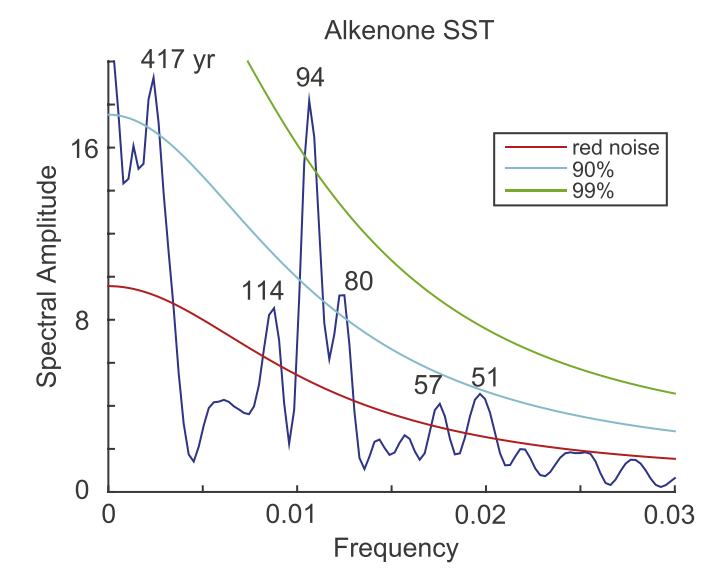
The study area is characterised by an extremely high sedimentation rate of approximately 0.5 cm/yr, making the site ideal for a highresolution study of past surface temperature changes. The entire core covers the last 1900 years (Fig. 2). However, the variability in accumulation rate of the core indicates a distinctive change in accumulation rate at a depth of 340 cm, corresponding to the year 1453 CE (Fig. 2). The mean value of the accumulation rate was 1-2 yr/cm ( $\pm 1.8-3, 1\sigma$ ) after 1453 CE, whereas it was 4–8 vr/cm ( $\pm 6$ –13, 1 $\sigma$ ) before 1453 CE. Hence, the sedimentation rates are different, at approximately 1-0.5 cm/yr for the upper part of the core and 0.1 cm/yr for the lower part. Alkenone temperature resolution is approximately 2-4 years for the upper part and 6-8 years for the lower part. The Bayesian statisticsbased age-depth model indicates that the uncertainties in the ages of sediments younger than 1453 CE are relatively small ( $\pm 10$ –20 yr), while the uncertainties in the ages of older sediments are large ( $\pm 16$ –40 yr) (top panel in Fig. 3).

For comparisons of alkenone SST record with other paleoclimatic records, we calculate correlation coefficients between them by using the Ebisuzaki method which is suitable for a serial correlation analysis. This method was conducted by implementing the 'surrogateCor' function in the R package 'astrochron' (Ebisuzaki, 1997; Meyers, 2014; Baddouh et al., 2016) with 10,000 Monte Carlo simulations.

# 3. Results

A new high-resolution alkenone SST record for the last 2 k was constructed by combining records from cores TY2010 PC4 and ARA/ES 03–01 GC01. The core-top temperature estimated from the  $U_{37}^{K'}$  value was 20.5 °C. A comparison with the 12-year averaged SSTs measured in situ (2000-2012) showed that the core-top alkenone temperature is higher than the observed annual mean SST (17.7  $^{\circ}$ C), and that it is close to the observed temperatures in June to October (Fig. 1). A bi-monthly record of total C<sub>37</sub> alkenone concentrations measured from suspended particles in surface waters at the core site shows that the concentration is the highest during summer (Fig. 1), indicating that the alkenones are predominantly produced in summer (Lee et al., 2014). In addition, alkenone analysis of the subsurface samples from the in situ bottle casts show that the concentration of total C<sub>37</sub> alkenones was typically high in the surface mixed layer and decreased with depth, indicating that alkenones were most likely produced in the surface mixed layer and thus that alkenone records from marine sediments represent near-surface signals (Lee et al., 2014).

Temporal variations in alkenone SSTs exhibited millennial evolution and fluctuations on multi-decadal to centennial timescales during the last 2 k (Fig. 3a). The increase in temperature since the mid-19th century is clear, which is associated with an anthropogenically induced global warming trend (IPCC, 2013). During the first of the two millennia, alkenone temperatures fluctuated between 19.4 °C and 21 °C. A cooler period occurred between 850 CE and 1200 CE. Hence, the Medieval Climate Anomaly interval (approximately 950–1250 CE) is not reflected



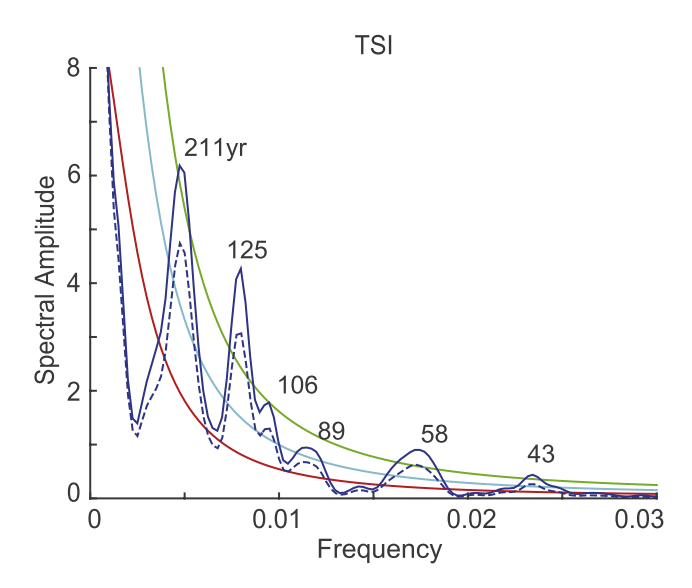


**Fig. 5.** Spectrum analysis of alkenone temperature (this study) and TSI (Roth and Joos, 2013) for the last 2 k. Time series of 10-year averaged alkenone temperature were used. For TSI time series, both 1-year resolution (line) and 10-year averaged (dashed line) TSI values were used.

**Table 3**Correlation coefficients between the reconstructed SST and TSI.

	Reconstructed SST & TSI <sup>a</sup>			
Period	140–2000	1200-2000	1500-2000	1600–2000
Correlation coefficient	0.17 <sup>b</sup>	0.23 <sup>b</sup>	0.27 <sup>b</sup>	0.54 <sup>c</sup>

- <sup>a</sup>: The TSI data are from Roth and Joos (2013).
- b: 95% confidence level.
- c: 99% confidence level.

clearly in this record. During the last millennium, there were several pronounced cold periods (e.g. 1267--1280 CE and 1626--1629 CE), and a few strong cooling events were centred at around 1715 CE, 1820 CE, and 1910 CE. The lowest temperature (18.7 °C) occurred in approximately  $1267\pm28$  CE. Comparisons of alkenone temperatures with tree-ring-based temperature records from the Korean Peninsula for the period of 1640--1989 CE (Choi et al., 1992) revealed that the cooling events

identified from the tree ring data at 1690 CE, 1730 CE, 1840 CE, and 1910 CE are consistent with those identified in the alkenone temperature records. Our SST record was also compared to tree ring-based air temperatures in Asia (PAGES 2k Consortium, 2013). A long-term cooling trend in the synthesised surface temperature in Asia beginning in approximately 1200 CE is consistent with that of our SST record (Fig. 3a and c).

Our record reveals that climate variability increased during the last millennium, especially in the period of 1200-1850 CE, relative to the preceding period of 500–1200 CE. SST variations range within  $\sim\!3\,^{\circ}\text{C}$ over the period of 1200–1850 CE and  $\sim 1\,^{\circ}\text{C}$  over 500–1200 CE (Fig. 3a). In this study, we used 10-year averaged SST for the entire period of the last 2 k to overcome the issue of time resolution of the record. It should be noted that even though the record for the last millennium is smoothed so as to emulate the resolution of the record for the first millennium, the increased variability in SST is still identified for the last millennium. During the period of 1200-1850 CE, cold and hot extremes (deviations of over  $1\sigma$ ) were more frequent. The magnitude of the running standard deviation (100-year window) was larger over 1200–1850 CE than over the earlier period (Fig. 3b). We investigated changes in the accumulation rate to ascertain whether the enhanced and rapid climate changes were associated with the sediment deposition rate. The accumulation rate of the upper part of the core (1-2 yr/cm after 1453 CE) was different from that of the lower part (4-8 yr/cm). We do not exclude the possibility that the enhanced variability in the alkenone SST of the upper part of the core is related to changes in the accumulation rate. However, the greatest variability in the SST running standard deviation occurred over 1200–1450 CE, which corresponds to a period of low sedimentation rates. The lowest temperature also occurred during this interval. These results indicate that the enhanced and rapid climate changes were not simply due to an increase in sedimentation rate. This suggests that, although the alkenone SST variability of the lower part of the core can be smoothed to some extent due to the low sedimentation rate, cold events and rapid climate changes are still recognisable.

We compared our alkenone temperature record to records of solar irradiation and volcanic activity covering the last 2k to examine the extent to which alkenone SST changes are correlated with changes in these phenomena (Fig. 4a, b, c). The total solar irradiation (TSI) data for the last 2 k used in the study were reconstructed based on radiocarbon production and solar activity instrumental data (Roth and Joos, 2013). According to the record, the overall solar irradiance for the first millennium of this period was stronger than that of the last millennium. Four distinct grand solar minima known as the Oort (1040-1080 CE), Wolf (1280-1350 CE), Maunder (1645-1715 CE), and Dalton (1790-1820 CE) were identified within the last millennium (Steinhilber and Beer, 2011). The minima appear to be correlated with the cold alkenone temperatures of the study area, considering the age uncertainty (Fig. 4b and c). However, variations in TSI did not always coincide with variations in alkenone SST, such as during the Spoerer period (1460–1550 CE) (Fig. 4b and c). In addition, the minimum in the temperature record apparently precedes the minimum in solar activity (Fig. 4b and c). Spectrum analysis was performed on both time series of alkenone temperature and TSI for the last 2 k. There are discrepancies in the periodicity of spectral peaks between the two time series (Fig. 5). However, at centennial time scale, significant peaks in the SST record are 94-year and 80-year, and those in TSI are 106-year and 89-year, respectively (Fig. 5). There might be some coherence between them (94-year and 80-year versus 106-year and 89-year). The differences are within the range of  $\pm 10\%$ . This may indicate that the solar forcing influence on the SST variability considering the uncertainty in each dataset. We also calculated the correlation coefficient between the reconstructed SST and the TSI (Table 3). The correlation is not significant for the entire period, but it becomes large (0.54 at 99% confidence level) when the period is confined to the last 400 years (1600-2000 CE). Although the correlation coefficient does not imply the causality, this

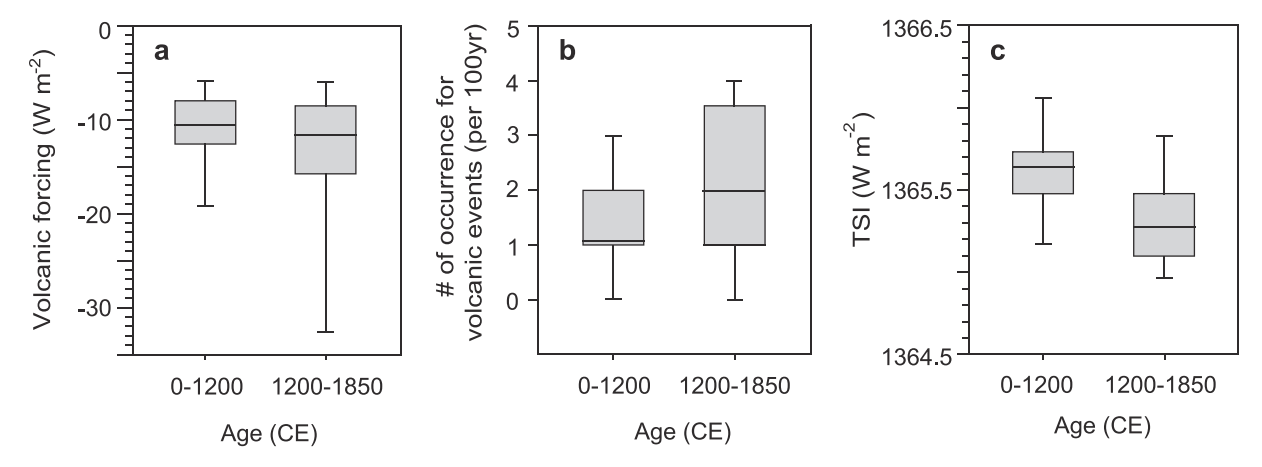


Fig. 6. Comparisons of (a) the intensity of volcanic forcing, (b) the number of occurrence of volcanic eruption per 100 years, and (c) the intensity of TSI between two periods (0–1200 CE and 1200–1850). The 32 largest volcanic events for the period of 0–1992 CE (Sigl et al., 2015) were used. TSI data for the last 2 k (Roth and Joos, 2013) were used. The box and whiskers denote the upper and lower quartiles, the median, and the minimum and maximum values.

result may indicate that the variability of solar forcing plays a role on the SST variability. However, in general, solar activity seems to be insufficient for explaining the entire SST cooling trend.

Previous studies have suggested that volcanic eruptions played an important role in climate variations (Sigl et al., 2015). The record of volcanic activity over the last 2 k was reconstructed based on atmospheric aerosol loading as measured in ice cores (Sigl et al., 2015). Comparisons of our SST temperature record with the atmospheric aerosol forcing record demonstrated that episodic cooling events identified in our record match with the volcanic activity record in terms of intensity and frequency within the error range of age determination (Fig. 4a and b). Overall, the magnitude of volcanic forcing ranges 8–12 W/m<sup>2</sup> for the first millennium, and 8–15 W/m<sup>2</sup> with the maximum of 32 W/m<sup>2</sup> for the second millennium (Fig. 6a). In addition, the number of occurrence of volcanic eruption significantly increased from the first to the second millennium (Fig. 6b). These imply that the volcanic forcing may significantly contribute to influence the enhanced SST variability during the second millennium. On the other hand, changes in total solar irradiance range less than  $\sim 1 \text{ W/m}^2$  over the last 2 k (Fig. 6c). Hence, the impact of volcanic forcing on surface temperature would be greater than that of solar insolation forcing. In particular, a tropical volcanic eruption in 1258 CE (Samalas Volcano, Indonesia) (Lavigne et al., 2013) correlated with an event-like cooling observed in our record. Although the Bayesian statistics-based age-depth model indicated an age uncertainty of  $\pm 28$  yr for the period of 1267–1280 CE, the timing of the cooling event is consistent with that of the volcanic activity. Furthermore, the increased frequency of volcanic events over the interval of 1258–1286 CE may be related to abnormally strong cooling during the time period, indicating a large contribution of volcanic activity toward climate changes. These observations are consistent with previous results, demonstrating that strong and frequent volcanic eruptions in the tropics and at high latitudes could have been primary drivers of interannual to decadal temperature variability in the Northern Hemisphere throughout the past 2 k (Sigl et al., 2015).

It is also noteworthy that Earth system model simulations indicate the surface cooling of East Asia in summer after large volcanic eruptions (Man et al., 2014). According to these simulations, the cooling appeared to be proportional to the magnitude of the volcanic forcing, and it persisted for a few years after some of the largest eruptive episodes. The cooling in 1258 CE could have begun in connection with volcanic activity, and it lasted several decades in connection with the Wolf solar minimum. Hence, the enhanced climate variability becomes evident when a volcanic forcing is accompanied by grand solar minimum and the occurrence of volcanic eruption increases for the time period. In contrast, the reconstruction of greenhouse gas (CO<sub>2</sub>, CH<sub>4</sub>, and N<sub>2</sub>O)

forcing levels from ice core data (MacFarling Meure et al., 2006; Joos and Spahni, 2008) showed that the response of SST to greenhouse gas forcing seemed to be less significant during this time period (Fig. 4d).

### 4. Discussion

Our alkenone SST record was obtained from one location in the northwestern subtropical Pacific margin. To examine how this record may represent a regional SST pattern, the alkenone SST data were compared with instrumental datasets including extended-reconstructed SST (ERSST v4, Huang et al., 2014) and the Hadley Centre Sea Ice and SST dataset (HadISST, Rayner et al., 2003) for 1870-2010. Fig. 7a shows the time series of the alkenone SST along with the averaged SST over June to October from the ERSSTv4 and HadISST datasets covering the past 140 years. It was found that the records are comparable with one another. To further examine the regional SST pattern associated with the alkenone SST record, we calculated regressed SST anomalies against the alkenone temperature by using the 11-year running mean SST of the HadISST dataset, since the age resolution of the alkenone temperature and the timescale of interest are greater than one year. The regression map of HadISST and alkenone temperatures (Fig. 7b) shows that the correlation with local SST is strong. The regressed SST anomalies against alkenone temperatures were characterised by a relatively good relationship along the subtropical western boundary current in the North Pacific. This indicates that SST changes identified at our study site are representative of those of the North Pacific Ocean basin and the Kuroshio and the Kuroshio extension in particular. We also constructed the regression by using detrended SST to eliminate a global warming trend that would have dominated the spatial pattern over the last 140 years. The detrended SST regression pattern shown in Fig. 7c displays the PDOlike pattern, which is characterised by cooling in the central North Pacific and warming along the west coast of the USA (Mantua and Hare, 2002). This result indicates that the variability in SST at the core site tended to coincide with that of a PDO-like SST pattern and the PDO-like SST variability is enhanced in the last millennium than in the previous millennium.

A recently published alkenone SST record for the last 2 k of the eastern subtropical Pacific captures multi-decadal variations that may relate to the PDO (O'Mara et al., 2019). The alkenone temperature anomalies shown in Fig. 8a and b were constructed based on the 10-year averaged temperatures in consideration of the difference in data resolution bewteen the first and the second millennia. The correlation coefficient and statistical probability between our alkenone SSTs and those of O'Mara et al. (2019) for the last 2 k were calculated. It was difficult to present statistically meaningful correlations for the last 2 k. This is

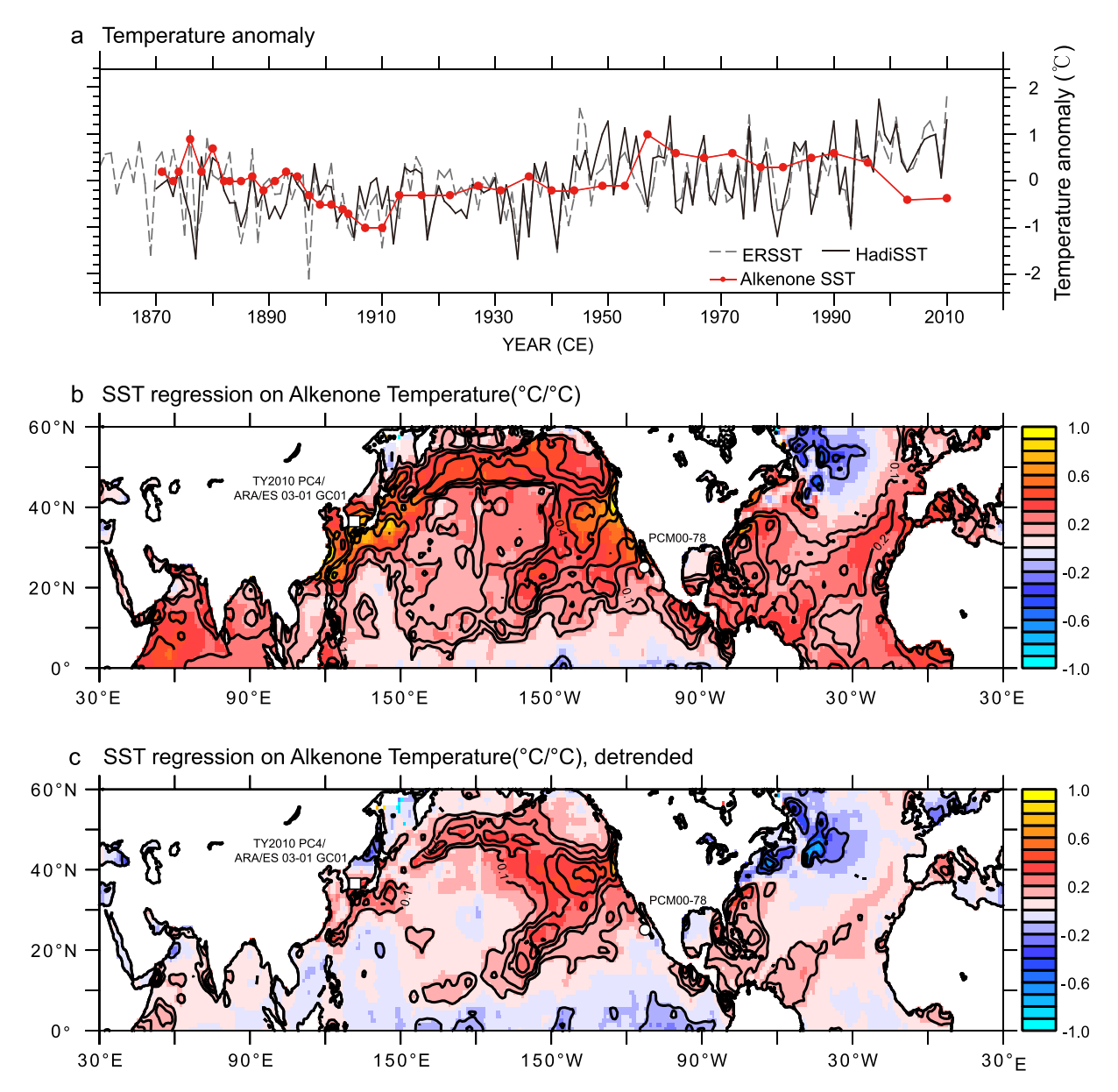


Fig. 7. (a) June to October temperature time series of ERSST (Huang et al., 2014) and HadISST (Rayner et al., 2003) near the core location (130°E, 36°N) and alkenone temperature for the period of 1870–2010 CE, Regression map of HadISST data and alkenone temperature with (b) 11-year running mean temperatures, and (c) detrended temperatures. The HadISST data are from Rayner et al. (2003).

probably either because the PDO pattern is not stationary, or because the age uncertainty is large. However, there seem to be opposite temperature patterns on the multi-decadal and centennial time scales. For examples, for the intervals centred at 500 CE and 750 CE, the western Pacific region was relatively warm, while the eastern Pacific region predominantly cooled. During the period of 1600–1700 CE, it was cold in the west, and warm in the east. Since 1800 CE, warming has been dominant in the west, and cooling has dominated in the east. In addition, the running standard deviation patterns of both alkenone records for a 100-year sliding window were consistent for the last millennium (Fig. 8c), indicating that both records contain enhanced multi-decadal to centennial variations during the period of 1200–1850 CE.

In this study, changes in the reconstructed SST were compared to the evolution of the East Asian summer monsoon system over the last 2 k (Fig. 9). Recent studies on variability in the East Asia summer monsoon (EASM) (Chiang et al., 2017; Liu et al., 2014; Zhang et al., 2018) showed that the EASM system undergoes complex spatio-temporal evolution. For example, the variability of a tripole mode of rainfall anomalies, which is

characterised by a drier central-to-eastern China and a wetter southern and northern China, is dominant in East Asia during the boreal summer on an interannual timescale. When the rainfall anomalies from NOAA dataset (Chen et al., 2002) were statistically regressed against the instrumental SST (i.e. HadISST) of our study area over the last 71 years, the tripole mode pattern was also exhibited (Fig. 9a). In general, Chinese cave  $\delta^{\bar{1}8}\text{O}$  signals reflect regional rainfall in East Asia, where higher EASM rainfall corresponds to more-depleted  $\delta^{18}O$  (e.g. Cheng et al., 2009). Time series of 10-year averaged alkenone temperature and Chinese cave  $\delta^{18}$ O records for the last 2 k were compared with each other. The Wanxiang stalagmite  $\delta^{18}$ O record from near the upper Yangtze River (Zhang et al., 2008) contains light values (corresponding to increased rainfall) for the periods of 400-700 CE and heavy values (decreased rainfall/drought) for the period of 1300–1800 CE (Fig. 9b). The correlation coefficient between our SST record and the cave monsoon record for the period of 1200–1850 CE is significantly high (r = -0.34, P = 0.003). On the other hand, the stalagmite  $\delta^{18}$ O record from Dongge cave (Wang et al., 2005), located in South China, exhibits heavy values (decreased rainfall/

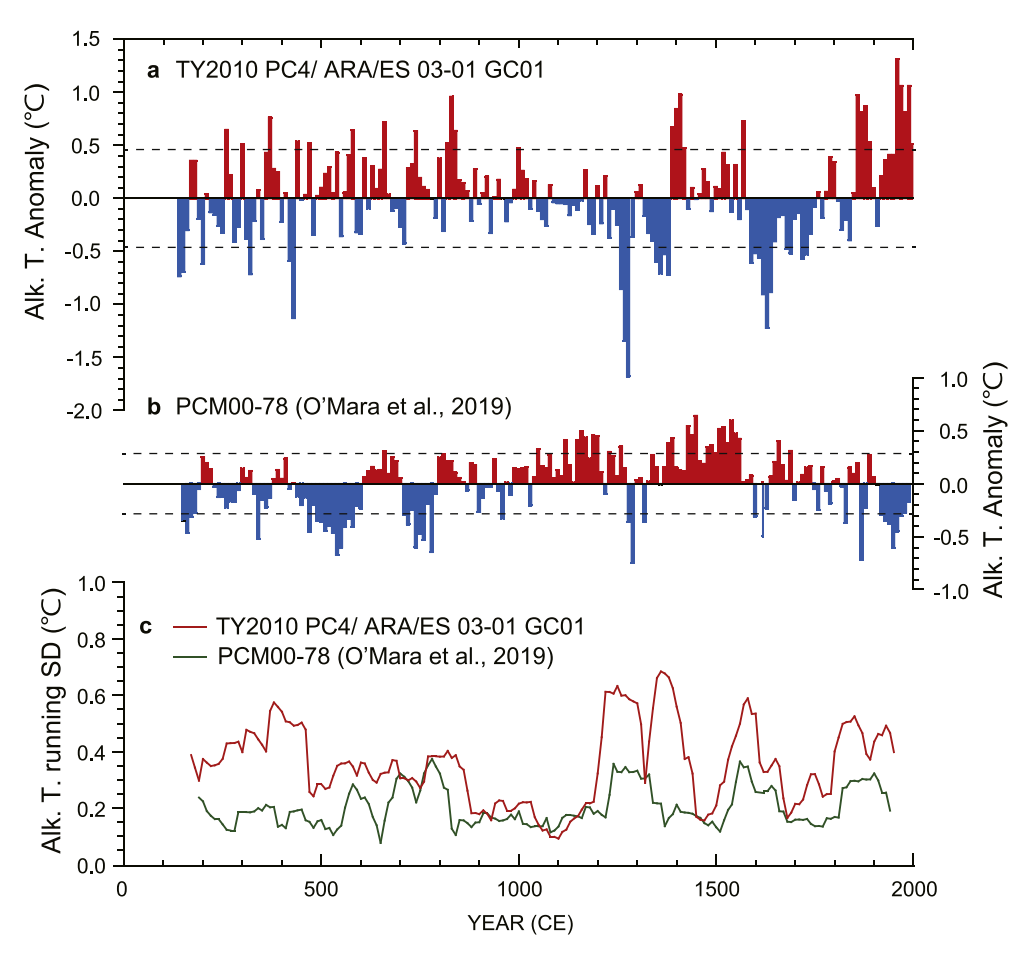


Fig. 8. Time series of 10-year averaged alkenone temperature of (a) our TY2010 PC4 / ARA/ES 03–01 GC01 cores from the western Pacific margin, (b) PCM00–78 core from the eastern Pacific margin (Baja California) (O'Mara et al., 2019), and (c) running standard deviation (100-year window) of our alkenone temperatures and those of O'Mara et al. (2019). The horizontal line indicates the mean value of each record for 2 k. Dashed lines represent intervals of the standard deviation, 1σ.

drought) for the periods of 400–700 CE and less-heavy and light values (increased rainfall) for the periods of 1400–1600 CE and 1700–1900 CE, respectively (Fig. 9e). Hence, the rainfall/drought patterns of the Wanxiang and Dongge are in opposition. The stalagmite  $\delta^{18}$ O record from Shenqi cave (Tan et al., 2018) shows a pattern different from that of the Wanxiang record, as indicated by the correlation coefficient ( $r\!=\!0.4,$   $p\!=\!0.03$ ) (Fig. 9c). The record from Heshang cave (Hu et al., 2008) does not show a clear pattern (Fig. 9d). The complicated patterns exhibited in the stalagmite  $\delta^{18}$ O records seem to be associated with variations in the tripole mode of the EASM-related rainfall in China, given that the cave  $\delta^{18}$ O records indicate regional rainfall.

For the period of 400–700 CE, EASM-related precipitation increased, and pluvials may have dominated near the upper Yangtze River. The light values given in the Wanxiang stalagmite  $\delta^{18} O$  record support this theory. Relatively warm SSTs at our core site appear to also be correlated with this pattern. However, southern China experienced drought in this period. For the period of 1400–1600 CE, drought prevailed across China (Cook et al., 2010), which is also supported by all cave records. Severe drought near the upper Yangtze River around 1600–1700 CE was linked to strong cooling at our core site. A seawater  $\delta^{18} O$  record covering 1300 years that was reconstructed using foraminiferal  $\delta^{18} O$  and alkenone temperature data from near our core site displayed a pattern similar to that of the Wanxiang stalagmite  $\delta^{18} O$  record (Lee and Park, 2015). It is noteworthy that the rainfall increased in the south of China in the period of 1700–1900 CE, as indicated by the Dongge stalagmite  $\delta^{18} O$  record. The alkenone SST in our record increased in the same

period. Overall, Chinese cave  $\delta^{18}$ O records revealed increased multi-decadal to centennial variability during the last millennium in comparison to that in the previous millennium.

# 5. Summary

The first well-preserved, high-resolution, continuous SST record of the northwestern Pacific margin spanning the past 2k revealed enhanced and rapid climate variability on multi-decadal to centennial timescales in the last millennium, which differed significantly from that in the previous millennium. A comparison of the SST record with volcanic and solar insolation records suggested that the enhanced variability in surface temperature was associated with changes in these phenomena, such as increased volcanic activity and grand solar minima during this period, implying that natural variability in these factors plays a role in increased regional climate variability. In addition, the reconstructed SST record at the core site represents the PDO-like variability, which is also enhanced in the last millennium than in the previous millennium. Comparisons of the SST record with  $\delta^{18}$ O records of Chinese caves revealed correlations between temperatures and the monsoon system over the past 2 k, suggesting that surface temperature extremes seem to be related to monsoon activity and hydrological cycle reinforcement in the upper Yangtze River with greater variability during the last millennium in comparison to that in the previous millennium.

Supplementary data to this article can be found online at https://doi.org/10.1016/j.gloplacha.2021.103558.

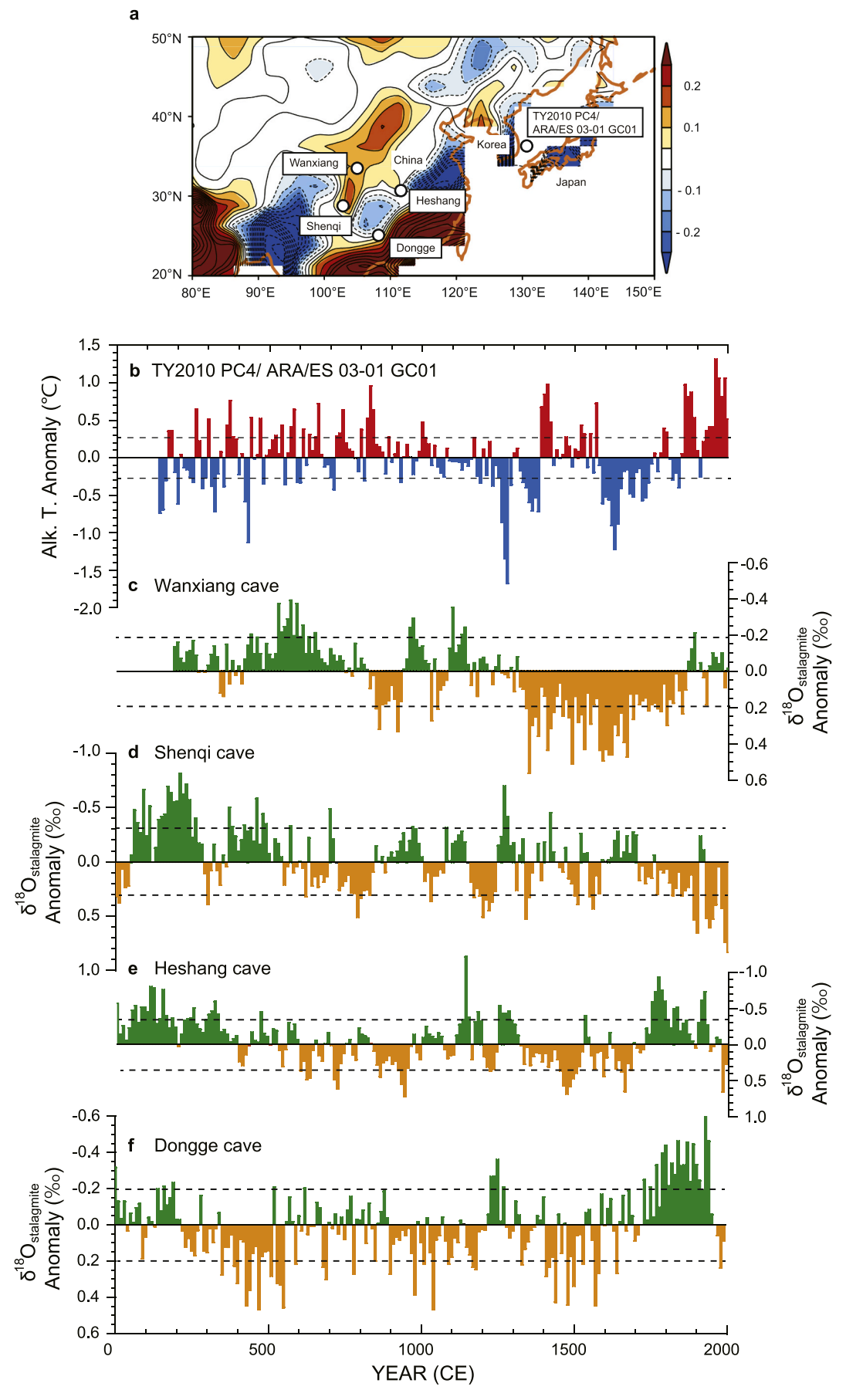


Fig. 9. (a) Rainfall anomalies regressed against instrumental SST (HadlSST) at the core site for the period of 1948–2019. The rainfall dataset was obtained from NOAA's PRECipitation REConstruction over Land (PREC/L, Chen et al., 2002). The circles indicate the location of cores and caves. Time series of 10-year averaged (b) alkenone temperature of our TY2010 PC4 / ARA/ES 03–01 GC01 cores in this study, (c) Wanxiang cave  $\delta^{18}$ O (Zhang et al., 2008), (d) Shenqi cave  $\delta^{18}$ O (Tan et al., 2018), (e) Heshang cave  $\delta^{18}$ O (Hu et al., 2008), and (f) Dongge cave  $\delta^{18}$ O (Wang et al., 2005). Horizontal lines indicate the mean value of each record for 2 k. Dashed lines represent intervals of the standard deviation 1σ.

# **Declaration of Competing Interest**

The authors declare that they have no known competing financial interests or personal relationships that could have appeared to influence the work reported in this paper.

# Acknowledgements

We thank reviewers and the Editor for their constructive comments and suggestions. This work was supported by a National Research Foundation of Korea grant funded by the South Korean government (Ministry of Science and ICT) (grant no. 2019R1A2C2004951) awarded to K.E. Lee. Paleoclimate proxy data relevant to this study are attached as Supplementary Information.

### References

- Baddouh, M., Meyers, S.R., Carroll, A.R., Beard, B.L., Johnson, C.M., 2016. Lacustrine  $^{87}\mathrm{Sr}/^{86}\mathrm{Sr}$  as a tracer to reconstruct Milankovitch forcing of the Eocene hydro-logic cycle. Earth Planet. Sci. Lett. 448, 62–68.
- Blaauw, M., Christen, J.A., 2011. Flexible paleoclimate age-depth models using an autoregressive gamma process. Bayesian Anal. 6 (3), 457–474.
- Chen, M., Xie, P., Janowiak, J.E., Arkin, P.A., 2002. Global land precipitation: a 50-yr monthly analysis based on gauge observations. J. Hydrometeorol. 3, 249–266.
- Cheng, H., Edwards, R.L., Broecker, W.S., Denton, G.H., Kong, X., Wang, Y., Zhang, R., Wang, X., 2009. Ice age terminations. Science 326, 248–252.
- Chiang, J.C.H., Swenson, L.M., Kong, W., 2017. Role of seasonal transitions and the westerlies in the interannual variability of the East Asian summer monsoon precipitation. Geophys. Res. Lett. 44, 3788–3795.
- Choi, J.N., Yu, K.B., Park, W.K., 1992. Paleoclimate reconstruction for Chungbu mountainous region using tree-ring chronology. Korean J. Quat. Res. 6 (1), 21–32 (in Korean with English abstract).
- Cook, E.R., Anchukaitis, K.J., Buckley, B.M., D'Arrigo, R.D., Jacoby, G.C., Wright, W.E., 2010. Asian monsoon failure and megadrought during the last millennium. Science 328, 486, 489.
- Ebisuzaki, W., 1997. A method to estimate the statistical significance of a correlation when the data are serially correlated. J. Clim. 10, 2147–2153.
- Hu, C., Henderson, G.M., Huang, J., Xie, S., Sun, Y., Johnson, K.R., 2008. Quantification of Holocene Asian monsoon rainfall from spatially separated cave records. Earth Planet. Sci. Lett. 266, 221–232. https://doi.org/10.1016/j.epsl.2007.10.015.
- Huang, B., Banzon, V.F., Freeman, E., Lawrimore, J., Liu, W., Peterson, T.C., Smith, T.M., Thorne, P.W., Woodruff, S.D., Zhang, H.-M., 2014. Extended Reconstructed Sea Surface Temperature version 4 (ERSST.v4): part I. upgrades and intercomparisons. J. Clim. 28, 911–930.
- IPCC, 2013. Climate Change 2013: The Physical Science Basis. In: Stocker, T.F., Qin, D., Plattner, G.-K., Tignor, M., Allen, S.K., Boschung, J., Midgley, P.M. (Eds.), Contribution of Working Group I to the Fifth Assessment Report of the Intergovernmental Panel on climate Change. Cambridge Univ. Press, Cambridge, United Kingdom and New York, NY, USA, p. 1535.
- Joos, F., Spahni, R., 2008. Rates of change in natural and anthropogenic radiative forcing over the past 20,000 years. Proc. Natl. Acad. Sci. 105, 1425–1430.
- Lavigne, F., Degeai, J.-P., Komorowski, J.-C., Guillet, S., Robert, V., Lahitte, P., Oppenheimer, C., Stoffel, M., Vidal, C.M., Surono, P.I., Wassmer, P., Hajdas, I., Hadmoko, D.S., de Belizal, E., 2013. Source of the great A.D. 1257 mystery eruption unveiled, Samalas volcano, Rinjani Volcanic Complex, Indonesia. Proc. Natl. Acad. Sci. 110, 16742–16747.
- Lee, K.E., Park, W., 2015. Initiation of East Asia monsoon failure at the climate transition from the Medieval Climate Anomaly to the Little Ice Age. Glob. Planet. Chang. 128, 83–89.
- Lee, K.E., Lee, S., Park, Y., Lee, H.J., Harada, N., 2014. Alkenone production in the East Sea/Japan Sea. Cont. Shelf Res. 74, 1–10.
- Liu, Z., Wen, X., Brady, E.C., Otto-Bliesner, B., Yu, G., Lu, H., Cheng, H., Wang, Y., Zheng, W., Ding, Y., Edwards, R.L., Cheng, J., Liu, W., Yang, H., 2014. Chinese cave records and the East Asia Summer Monsoon. Quat. Sci. Rev. 83, 115–128. https://doi.org/10.1016/j.quascirev.2013.10.021.

- MacFarling Meure, C., Etheridge, D., Trudinger, C., Steele, P., Langenfelds, R., van Ommen, T., Smith, A., Elkins, J., 2006. Law Dome CO<sub>2</sub>, CH<sub>4</sub> and N<sub>2</sub>O ice core records extended to 2000 years BP. Geophys. Res. Lett. 33, L14810.
- Man, W., Zhou, T., Jungclaus, J.H., 2014. Effects of large volcanic eruptions on global summer climate and East Asian monsoon changes during the last millennium: analysis of MPI-ESM simulations. J. Clim. 27, 7394–7409.
- Mantua, N.J., Hare, S.R., 2002. The Pacific Decadal Oscillation. J. Oceanogr. 58, 35–44.
  McGregor, H.V., Evans, M.N., Goosse, H., Leduc, G., Martrat, B., Addison, J.A.,
  Mortyn, P.G., Oppo, D.W., Seidenkrantz, M.-S., Sicre, M.-A., Phipps, S.J.,
  Selvaraj, K., Thirumalai, K., Filipsson, H.L., Ersek, V., 2015. Robust global ocean
  cooling trend for the pre-industrial Common Fra. Nat. Geosci. 8, 671–677.
- Meyers, S.R., 2014. Astrochron: An R Package for Astrochronology. https://cran. r-project.org/package=astrochron.
- Müller, P.J., Kirst, G., Ruhland, G., von Storch, I., Rosell-Melé, A., 1998. Calibration of the alkenone paleotemperature index U<sup>8</sup>/<sub>37</sub> based on core-tops from the eastern South Atlantic and the global ocean (60°N-60°S). Geochim. Cosmochim. Acta 62, 1757. 1772.
- O'Mara, N.A., Cheung, A.H., Kelly, C.S., Sandwick, S., Herbert, T.D., Russell, J.M., Abella-Gutiérrez, J., Dee, S.G., Swarzenski, P.W., Herguera, J.C., 2019. Subtropical Pacific Ocean temperature fluctuations in the Common Era: multidecadal variability and its relationship with Southwestern North American Megadroughts. Geophys. Res. Lett. 46 https://doi.org/10.1029/2019GL084828.
- PAGES 2k Consortium, 2013. Continental-scale temperature variability during the past two millennia. Nat. Geosci. 6, 339–346.
- Prahl, F.G., Wakeham, S.G., 1987. Calibration of unsaturation patterns in long-chain ketone compositions for palaeotemperature assessment. Nature 330, 367–369.
- Prahl, F.G., Muehlhausen, L.A., Zahnle, D.L., 1988. Further evaluation of long-chain alkenones as indicators of paleoceanographic conditions. Geochim. Cosmochim. Acta 52, 2303–2310.
- Prahl, F.G., Collier, R.B., Dymond, J., Lyle, M., Sparrow, M.A., 1993. A biomarker perspective on prymnesiophyte productivity in the northeast Pacific Ocean. Deep-sea Res. 40, 2061–2076.
- Rayner, N.A., Parker, D.E., Horton, E.B., Folland, C.K., Alexander, L.V., Rowell, D.P., Kent, E.C., Kaplan, A., 2003. Global analyses of sea surface temperature, sea ice, and night marine air temperature since the late nineteenth century. J. Geophys. Res. 108, 4407
- Roth, R., Joos, F., 2013. A reconstruction of radiocarbon production and total solar irradiance from the Holocene <sup>14</sup>C and CO<sub>2</sub> records: implications of data and model uncertainties. Clim. Past 9, 1879–1909.
- Sigl, M., Winstrup, M., McConnell, J.R., Welten, K.C., Plunkett, G., Ludlow, F., Büntgen, U., Caffee, M., Chellman, N., Dahl-Jensen, D., Fischer, H., Kipfstuhl, S., Kostick, C., Maselli, O.J., Mekhaldi, F., Mulvaney, R., Muscheler, R., Pasteris, D.R., Pilcher, J.R., Salzer, M., Schüpbach, S., Steffensen, J.P., Vinther, B.M., Woodruff, T. E., 2015. Timing and climate forcing of volcanic eruptions for the past 2,500 years. Nature 523, 543–549.
- Skinner, L.C., McCave, I.N., 2003. Analysis and modeling of gravity- and piston coring based on soil mechanics. Mar. Geol. 199, 181–204.
- Steinhilber, F., Beer, J., 2011. Solar activity the past 1200 years. PAGES News 19, 5–6.
- Tan, L., Cai, Y., Cheng, H., Edwards, R.L., Lan, J., Zhang, H., Li, D., Ma, L., Zhao, P., Gao, Y., 2018. High resolution monsoon precipitation changes on southeastern Tibetan Plateau over the past 2300 years. Quat. Sci. Rev. 195, 122–132. https://doi.org/10.1016/j.quascirev.2018.07.021.
- Tierney, J.E., Tingley, M.P., 2018. BAYSPLINE: a new calibration for the alkenone paleothermometer. Paleoceanogr. Paleoclimatol. 33, 281–301.
- Wang, Y., Cheng, H., Edwards, R.L., He, Y., Kong, X., An, Z., Wu, J., Kelly, M.J., Dykoski, C., Li, X., 2005. The Holocene Asian monsoon: links to solar changes and North Atlantic climate. Science 308, 854–857. https://doi.org/10.1126/ science.1106296.
- Wang, J., Yang, B., Ljungqvist, F.C., Luterbacher, J., Osborn, T.J., Briffa, K.R., Zorita, E., 2017. Internal and external forcing of multi-decadal Atlantic climate variability over the past 1,200 years. Nat. Geosci. 10, 512–517.
- Zhang, P., Cheng, H., Edwards, R.L., Chen, F., Wang, Y., Yang, X., Liu, J., Tan, M., Wang, X., Liu, J., An, C., Dai, Z., Zhou, J., Zhang, D., Jia, J., Jin, L., Johnson, K.R., 2008. A test of climate, sun, and culture relationships from an 1810-year Chinese cave record. Science 322, 940–942.
- Zhang, H., Griffiths, M.L., Chiang, J.C.H., Kong, W., Wu, S., Atwood, A., Huang, J., Cheng, H., Ning, Y., Xie, S., 2018. East Asian hydroclimate modulated by the position of the westerlies during Termination I. Science 362, 580–583. https://doi. org/10.1126/science.aat/9393.